CrossMark

CONTAMINATED SITES, WASTE MANAGEMENT AND GREEN CHEMISTRY: NEW CHALLENGES FROM MONITORING TO REMEDIATION

Synthesis of rigid polyurethane foams from phosphorylated biopolyols

Juan Carlos de Haro[1] · Daniel López-Pedrajas[1] · Ángel Pérez[1] ·
Juan Francisco Rodríguez[1] · Manuel Carmona[1]

Abstract Renewable resources are playing a key role on the synthesis of biodegradable polyols. Moreover, the incorporation of covalently linked additives is increasing in importance in the polyurethane (PU) market. In this work, previously epoxidized grape seed oil and methyl oleate were transformed into phosphorylated biopolyols through an acid-catalyzed ring-opening hydrolysis in the presence of H_3PO_4. The formation of phosphate polyesters was confirmed by FT-IR and ^{31}P-NMR. However, the synthesis of a high-quality PU rigid foam was not possible using exclusively these polyols attending to their low hydroxyl value. In that way, different rigid PU foams were prepared from the phosphorylated biopolyols and the commercial polyol Alcupol R4520. It was observed that phosphorylated biopolyols can be incorporated up to a 57 wt.% in the PU synthesis without significant structural changes with respect to the commercial foam. Finally, thermogravimetric and EDAX analyses revealed an improvement of thermal stability by the formation of a protective phosphorocarbonaceous char layer.

✉ Manuel Carmona
Manuel.CFranco@uclm.es

1 Department of Chemical Engineering, Institute of Chemical and Environmental Technology, University of Castilla-La Mancha, Avda. Camilo José Cela s/n, 13071 Ciudad Real, Spain

Introduction

Polyurethanes (PUs) are versatile polymers which have traditionally been produced from petroleum (Avar et al. 2012). The PU products can be divided mainly into elastomers (Petrović and Ferguson 1991), adhesives (Bahattab et al. 2011), coatings (Chattopadhyay and Raju 2007), and foams (Narine et al. 2007). Over three quarters of the global consumption of PU products is in the form of foams (Zia et al. 2007). PU foams cover a wide range of applications, including thermal insulation, footwear, bedding, and automotive seating, etc. Most of the rigid PU foam currently available on the market are made from petroleum-based polyether or polyester polyol. However, growing concerns about biodegradability, sustainability, carbon dioxide emissions, and other environmental problems are driving the search of renewable raw materials to substitute petroleum in polyol production (Petrovic 2008; Vroman and Tighzert 2009).

Vegetable oils and related products (e.g., free fatty acids) are non-toxic, non-volatile, renewable, and biodegradable resources which represent the main biomaterial for the synthesis of biopolyols and other chemicals (Grishchuk and Karger-Kocsis 2011; Islam et al. 2014; Liu et al. 2012b). There are several methods to prepare vegetable oil-based polyols: thiol-ene coupling reaction (Samuelsson et al. 2004), ozonolysis (Petrović et al. 2005), hydroformylation (Petrović et al. 2008), transesterification (Tavares et al. 2016), etc., being the epoxidation of the double bonds and their further hydrolysis the most important pathway (Miao et al. 2014). Different functional groups, such as ester (Fridrihsone et al. 2013), acyl (Sharma et al. 2008), azide (de Haro et al. 2016b), or amine groups (Biswas et al. 2005), have been incorporated into biopolyols using this route.

Among the different vegetable oils, grape seed oil is a highly unsaturated one which can be obtained by pressing or solvent

extraction from grape seeds (Da Porto et al. 2013; Sovová et al. 1994; Venkitasamy et al. 2014). Despite that it is an edible oil, it can be considered as a by-product of winemaking industry since the potential production of grape seed oil is huge compared with its average consumption as edible oil (Ng et al. 2015). This causes grape seed to be burned as biofuel for energy production (Fiori et al. 2012). Moreover, many authors defend that grape seed oil does not belong to the high nutritional oil group due to its fatty acid profile and low content of vitamin E active compounds (Matthäus 2008; Shinagawa et al. 2015).

The epoxides are cyclic ethers which generate a great tension in the molecule, increasing the reactivity of the vegetable oils. The most extended and well epoxidation route is the Prilezhaev method (Findley et al. 1945), in which reaction mechanism and the kinetic model have already been proposed on literature (de Haro et al. 2016a; Goud et al. 2006).

However, most PU are in general very flammable which is a highly undesirable characteristic under burning conditions because it represents a risk for the security. In that way, during the synthesis of a PU foams, beside the polyol and polyisocyanate, different additives are incorporated to improve the quality of the final product. Flame retardants, which are considered as one of the most important additives, inhibit or delay the spread of thermal decomposition by suppressing the combustion cycle on the surface of the material. There are two different approaches to incorporate flame retardants in PU foams either as free additives or as functional groups grafted covalently to the polyol/polyisocyanate structure. The latter one offers several advantages, such that functional groups are not susceptible to be lost through migration to the polymer surface of solvent leaching, what can become an environment problem (Chokwe et al. 2015; Kim et al. 2013; Pereira et al. 2015). Also, it can be homogeneously dispersed throughout the polymer and because of this may be required lower concentrations of additives than comparable not grafted ones (Chattopadhyay and Webster 2009). Several reactive flame retardants have been proposed, being phosphorus compounds the most important group of environmentally friendly flame retardant due to its low toxicity, no release of poison gases and producing low smoke during the burning process (Levchik and Weil 2006; van der Veen and de Boer 2012).

The goals of this work were focused on the synthesis of different phosphorylated biopolyols that could act as flame retardants and further to study the technical viability of synthesizing rigid PU foams using these biopolyols. Grape seed oil and the oleic acid were chosen as raw materials because they actually represent the two main by-products generated by the wine and edible oil industries, respectively, at the region of Castilla-La Mancha (Spain). The epoxidation of both raw materials and the subsequent hydrolysis reaction in presence of phosphoric acid were studied. Finally, the synthesis of rigid PU foams with enhanced thermal stability properties was accomplished.

Materials and methods

Materials

Grape seed oil was provided by Bodegas Crisve, a local co-operative from Ciudad Real (Spain). Methyl oleate was produced from oleic acid (technical grade, >90%) and methanol (>99%) supplied by Sigma-Aldrich using the method indicated at EN ISO 12966-2:2011. Glacial acetic acid (CH_3COOH, 99–100%), sulfuric acid (H_2SO_4, 95–97%), aqueous hydrogen peroxide (H_2O_2, 50 wt.%), phosphoric acid (H_3PO_4, 85%), potassium iodide (KI, 99.5–100%), hydrogen bromide solution in acetic acid (HBr, 33 wt.%), violet crystal (90–100%), potassium hydroxide (KOH, 0.5 M ethanolic dissolution), phenolphthalein ($C_{20}H_{14}O_4$, 1% in ethanol), potassium hydroxide (KOH 0.1 N ethanolic dissolution), tetrahydrofuran (THF, C_4H_8O, 99.9–100%), methyl nonadecanoate ($C_{19}H_{40}O_2$, 99.5–100%), and methylenediphenyldiisocyanate (MDI, 98%) were supplied by Sigma-Aldrich. Sodium thiosulfate ($Na_2S_2O_3 \cdot 5H_2O$, 0.1 M), cyclohexane (C_6H_{12}, 99.5–100%), Wij's reactive (0.1 N), potassium hydrogen phthalate ($C_6H_4COOHCOOK$, 99.8–100%), pyridine (C_5H_5N, 99.5–100%), acetic anhydride (($CH_3CO)_2$, 98–100%), ethanol (CH_3CH_2OH, 96%), and diethylether ($C_2H_5OC_2H_5$, 99.7–100%) were supplied by Panreac. Methanesulfonic acid (Lutropur MSA100) was supplied by BASF. The commercial polyol Alcupol R4520 (molecular weight 5500 g/mol; hydroxyl value 455 mg KOH/g) was supplied by Repsol. Methylene diphenyl diisocyanate (MDI) was supplied by Poliuretanos Aismar, S.A. The catalyst Tegoamin 33 and the silicone Tegostab B8404 were supplied by Evonik Degussa International AG. All the reagents were used as received without any further purification.

Epoxidation procedure

The epoxidation reaction was performed in a 1-l mechanically agitated glass reactor equipped with a six-bladed Rushton stainless steel stirrer according to an optimized method studied previously (de Haro et al. 2016a). For this purpose, the required amount of grape seed oil or methyl oleate and 0.5 mol of acetic acid per mole of unsaturation were added to the reactor. Then, the agitation rate and temperature were fixed at the desired values. Once the bulk reached the desired values, the catalyst (H_2SO_4, 2% by weight of the aqueous phase) and aqueous H_2O_2 (2 mol per mole of unsaturation) were added. H_2O_2 was introduced drop-wise over 30 min. The reaction was performed at 90 °C for 60 min.

Ring-opening reaction procedure

All the hydrolysis reactions reported in this study were carried out in a multi-neck round-bottom 500-ml reactor equipped

Table 1 Iodine value, oxirane oxygen content, hydroxyl values, conversion, and yield towards epoxide groups of the raw materials and the epoxidized products (epoxidation conditions: molar ratio acetic acid/H_2O_2/unsaturation = 0.5:2:1; H_2SO_4: 2% by weight of the aqueous phase; T = 90 °C; t = 60 min)

Sample	Iodine value (g I_2/100 g)	Oxirane oxygen (%)	Hydroxyl value (mg KOH/g)	Conversion (%)	Yield (%)
GSO	140.30	0.0	4	-	-
MO	88.37	0.0	4	-	-
EGSO	46.72	5.02	13	66.70	56.76
EMO	23.77	3.60	17	73.10	64.62

with a thermocouple, a magnetic stirrer, and a reflux condenser placed in an oil bath following the procedure indicated elsewhere (Guo et al. 2007). A mass ratio acetone/H_3PO_4/water/epoxidized product of 5:1:1:1 was used. The mixture was kept under reflux at 56 °C for 6 h. The obtained product was washed with ultrapure water to remove the H_3PO_4. Finally, the organic phase was separated by centrifugation, and the solvents were removed by vacuum evaporation.

Foaming procedure

Rigid PU foams were synthesized by weighting and mixing the desired masses of polyol, silicone, water, and amine catalyst. This mixture was agitated until a perfect homogenization was achieved. Then, the required amount of MDI was added and the resulting solution was stirred for 15 s, at which point the foam started to grow up. Finally, the foams were cured at room temperature. The required quantities of these reactants were calculated based on the hydroxyl number of the polyol used to synthesize the rigid PU foam, as indicated elsewhere (Simón et al. 2015).

Analytical techniques

Iodine value determinations were carried out according to EN 14111:2003 method. From this quantified value, the conversion of double bonds during the epoxidation reaction was calculated following the eq. 1.

$$Conversion\ (\%) = \frac{IV_0 - IV_f}{IV_0} \cdot 100 \qquad (1)$$

where IV_0 is the iodine value of the raw material and IV_f the iodine value of the epoxidized product.

The amount of oxirane oxygen (OO), expressed in percentage by weight, was calculated by direct method employing hydrobromic acid solution in glacial acetic acid according to AOCS Official Method Cd 9-57. This result was used to

determine the yield of the epoxidation process according to eq. 2.

$$Yield\ (\%) = \frac{OO \cdot \dfrac{253.8}{16}}{IV_0} \cdot 100 \qquad (2)$$

The hydroxyl value, in mg KOH per gram of product, was carried out according to the AOCS Official Method Tx 1a-66. Duplicate analyses were performed on each sample for all the variables and average values are reported.

The molecular weight distribution of each product was determined with gel permeation chromatography (GPC). Products were previously dissolved in THF at a concentration of 10 mg/ml. A Shimadzu chromatograph system (Japan) equipped with two columns (Styragel HR2 and Styragel HR0.5), using THF as the eluent at 40 °C (flow rate of 1 ml/min), and a refractive index detector was used.

The presence of phosphate esters and hydroxyl groups was determined using a Perkin-Elmer 16PC FT-IR spectrophotometer with 35 scans per sample at a resolution of 8 cm^{-1} in the range of 4000–400 cm^{-1}.

Phosphorus nuclear magnetic resonance spectroscopy (^{31}P-NMR) was measured with a Varian Gemini FT-400 spectrometer using chloroform as solvent. H_3PO_4 (85%, aqueous solution) was used for calibrating ^{31}P-NMR.

In order to study the flame retardant capability of the synthesized PU foams and biopolyols, thermogravimetric analyses were performed using a TA Instruments SDT Q600 Simultaneous DSC-TGA. Samples were heated from room temperature to 700 °C at a heating rate of 10 °C/min under a synthetic air atmosphere. The data were analyzed using TA Universal Analysis 200 software.

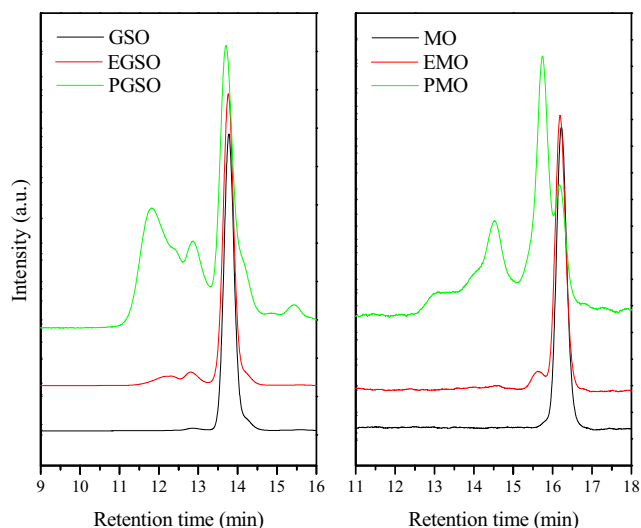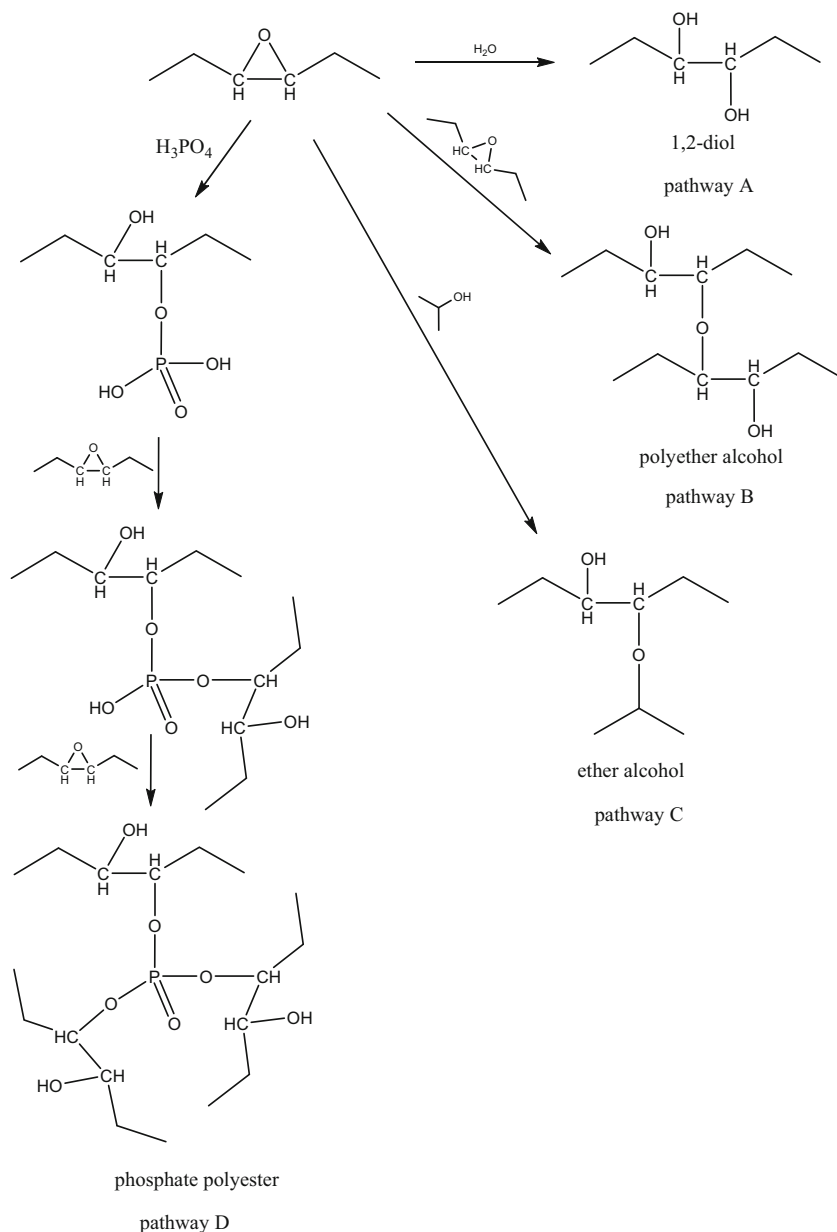The PU foams were also characterized using a Quanta 250 scanning electron microscope (SEM) to observe the cell

Fig. 1 GPC chromatogram showing the evolution of the MW distribution of the obtained products from GSO and MO

Fig. 2 Ring-opening pathways
of epoxides in presence of H_3PO_4
as acid catalyst

structure and its size distribution. It was coupled to an energy dispersive X-ray spectrometer (EDAX) for elemental composition analysis.

Results

Epoxidation reaction

The grape seed oil (GSO) and methyl oleate (MO) were characterized prior to epoxidation. Table 1 shows the iodine value and the hydroxyl value of both raw materials. The iodine value of both raw materials is similar to that of other compounds previously used in the literature to produce epoxidized biodegradable compounds (Ji et al. 2015; Lu et al. 2010). Hydroxyl and acid values are also in the average range. Therefore, it confirms that grape seed oil and methyl oleate are appropriate starting material for the biopolyol synthesis via epoxidation. The oxirane oxygen content (OO) of both raw materials was also determined, and as expected, they were free of this functional group.

GSO and MO were epoxidized following the previously indicated procedure. During the in situ epoxidation, the peracetic acid is generated from acetic acid and hydrogen
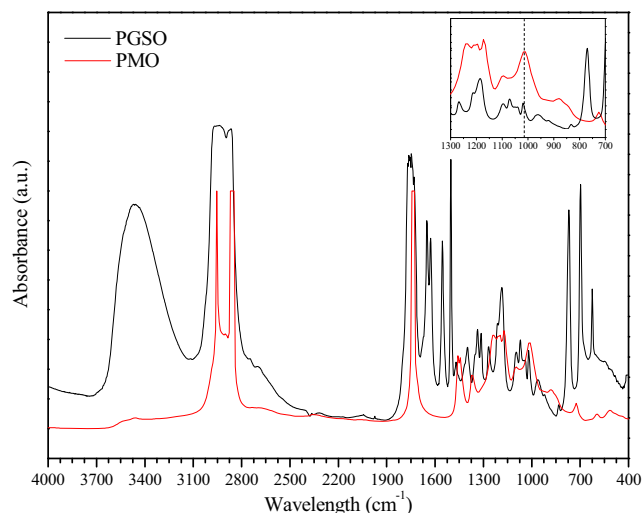
Fig. 3 FT-IR spectra of the PGSO and PMO

peroxide in the presence of sulfuric acid as catalyst. Acetic acid and sulfuric acid were chosen due to its higher catalytic activity (Dinda et al. 2008).

Table 1 shows the obtained iodine values, hydroxyl values, and oxirane oxygen content of the epoxidized grape seed oil (EGSO) and the epoxidized methyl oleate (EMO). The double-bond conversion and the yield of the process towards the formation of epoxy groups were calculated from these values as described in "Analytical techniques" section. As can be observed, the conversion of MO is greater than the conversion obtained in the case of GSO. The same trend was also observed in the case of the yield of the process to the formation of oxirane rings. This effect might be caused by the different steric hindrance of MO and GSO due to their different molecular weights and polarities.

The differences between the conversion and yield of the process on the epoxidation reaction for both raw materials indicate the presence of secondary reactions. As has been previously established in literature, the epoxide groups might be hydrolyzed to form hydroxyl groups. It was evident that
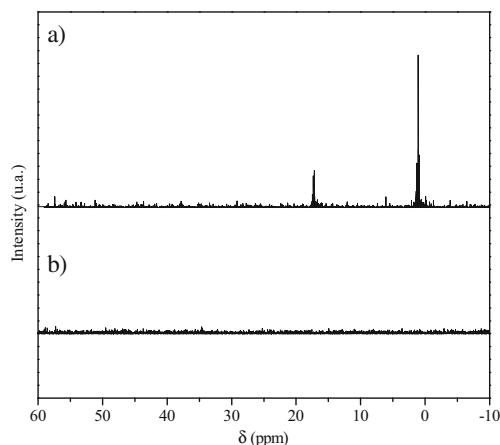

Fig. 4 ^{31}P-NMR spectra: **a** PGSO and **b** EGSO

this secondary reaction took place during the process based on the increase of hydroxyl value of the epoxidized products with respect to the raw materials. Besides, the hydroxyl groups can react with the epoxide groups previously formed, creating ether linkages to form oligomers (de Haro et al. 2016a; Guo et al. 2000). The presence of oligomers was confirmed by the GPC analyses (Fig. 1). As can be observed, EGSO and EMO chromatographs presented three peaks, which correspond to the main product, dimers, and trimers. In addition, a slight increase in MW of the main product of both epoxidized products was observed due to the incorporation of the oxirane oxygen to GSO and MO.

Ring-opening reaction with H_3PO_4

Figure 2 shows a general reaction mechanism for the acid-catalyzed ring-opening hydrolysis of oxirane compounds. As can be observed, a wide variety of species can be obtained as products. Wu and Soucek indicated that this reaction can lead to the formation of 1,2-diol compounds (pathway A), polyether alcohols (pathway B), and ether alcohols when phosphate ion does not participate on the reaction progress (Wu and Soucek 1998). However, Guo et al. have already reported that the use of H_3PO_4 as ring-opening agent might drive to the formation of phosphate mono-, di-, and triesters (pathway D) (Guo et al. 2007). Therefore, the four different pathways compete each other for the ring-opening reaction.

Both epoxidized products, EGSO and EMO, were hydrolyzed using H_3PO_4 as ring-opening agent. The obtained biopolyols were named as phosphorylated grape seed oil (PGSO) and phosphorylated methyl oleate (PMO). In both cases, the obtained products had an oxirane oxygen content of 0.0%, indicating a full conversion of the epoxy groups. The hydroxyl values of PGSO and PMO were found to be 123 and 45 mg KOH/g, respectively. As expected, these values increased during the hydrolysis reaction compared with it epoxidized precursor. However, the increase observed in the hydroxyl value of PGSO was much greater than PMO one. This can be explained by the fact that GSO has a higher steric hindrance than MO, and therefore, oligomerization reactions described previously (Fig. 2, pathways B, C, and D) are not favored during EGSO hydrolysis reaction. Figure 1 shows that the main specie after the hydrolysis reaction of PGSO was the triglyceride, contrary to the case of PMO which was the dimer. Nevertheless, a slight increase on the MW of all the species was observed due to the incorporation of the hydroxyl and phosphate groups. However, the identification of the different possible products was not possible due to the wide variety of formed species and the overlapping of their MWs, according to the GPC chromatogram (Fig. 2).

Figure 3 presents the FT-IR spectra of PGSO and PMO. The FT-IR spectra shows the characteristic bands of hydroxyl groups at 3480 cm^{-1}, C–H stretching vibrations at 2875–2970 cm^{-1}, –CH$_2$ and –CH$_3$ at 1350–1450 cm^{-1}. As hydroxyl

Table 2   Rigid PU foam composition

Foam	Component (wt.%)						
	R4520	PGSO	PMO	MDI	Water	Silicone	Catalyst
PU-PGSO	0.000	0.576	0.000	0.386	0.014	0.009	0.014
PU-PMO	0.0000	0.0000	0.6490	0.3088	0.0162	0.0097	0.0162
PU-R4520	0.4045	0.0000	0.0000	0.5692	0.0101	0.0061	0.0101
PU-A	0.0000	0.5113	0.0730	0.3776	0.0146	0.0088	0.0146
PU-B	0.1302	0.3907	0.0000	0.4452	0.0130	0.0078	0.0130
PU-C	0.1085	0.3254	0.1085	0.4224	0.0136	0.0081	0.0136
PU-D	0.0000	0.4283	0.1666	0.3664	0.0149	0.0089	0.0149
PU-E	0.0428	0.2231	0.3290	0.3664	0.0149	0.0089	0.0149
PU-F	0.1166	0.1832	0.2554	0.4086	0.0139	0.0083	0.0139
PU-G	0.1708	0.2226	0.1242	0.4488	0.0129	0.0078	0.0129
PU-H	0.2846	0.1708	0.0000	0.5151	0.0114	0.0068	0.0114
PU-I	0.2576	0.1288	0.0906	0.4920	0.0119	0.0072	0.0119
PU-J	0.2178	0.0861	0.2026	0.4607	0.0127	0.0076	0.0127
PU-K	0.0892	0.0000	0.5057	0.3663	0.0149	0.0089	0.0149
PU-L	0.1973	0.0000	0.3324	0.4359	0.0132	0.0079	0.0132
PU-M	0.3349	0.0000	0.1116	0.5245	0.0112	0.0067	0.0112

values predicted, the band of hydroxyl groups is much more intense at PGSO than at PMO. The presence of another characteristic signal at 1020 cm^{-1} is also remarkable indicating the presence of phosphate ester groups (Guo et al. 2007; Pretsch et al. 2000).

^{31}P-NMR spectroscopy, which is a more sensitive technique, was performed to confirm the incorporation of phosphorous into the structure of the biopolyol. Figure 4 shows the ^{31}P-NMR spectrum of PGSO (a) and EGSO (b). PGSO spectra present two signals at 1.02 and 17.23 ppm. This indicates that H$_3$PO$_4$ is attached to the skeleton of the bipolyol and that it is not present as a free molecule. Furthermore, the presence of two different chemical shifts indicates that two different phosphoric functional groups are linked. These signals were assigned to phosphate mono- and diester, according to Fig. 2 (pathway D), in which these products are easier formed than phosphate triester.

Assessment of PGSO and PMO in rigid PU foam synthesis

Different rigid PU foams were synthesized from PGSO and PMO as biopolyols. The commercial polyol Alcupol R4520 was used as reference material to compare the internal structure and flame retardant properties.

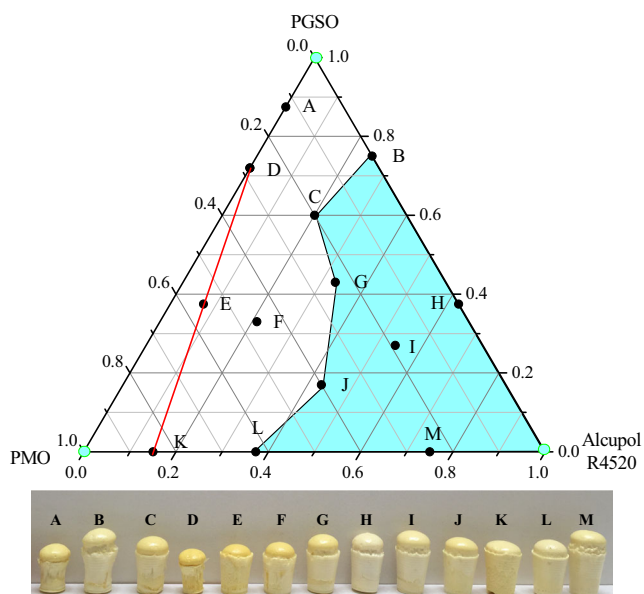**Fig. 5** SEM images of **a** PU-R4520 and **b** PU-PGSO
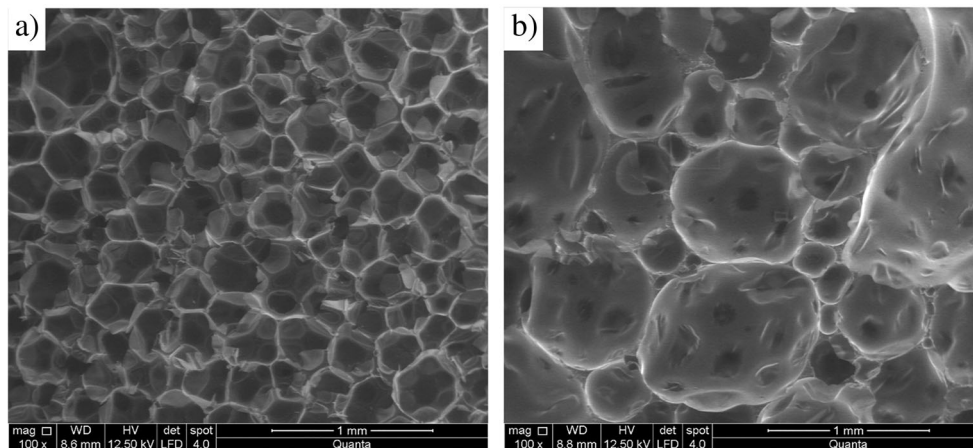
Fig. 6 Polyol mixture composition and physical aspect of the synthesized rigid PU foams

Fig. 8 TGA and DTGA curves of the rigid PU foams PU-R4520 and PU-J

Firstly, three different foams were produced using each one of these polyols. The amounts of reactants used on the synthesis are specified at Table 2. Unfortunately, the synthesis of a rigid PU foam using exclusively PMO was not possible due to its low hydroxyl value. Therefore, two rigid PU foams were obtained from PGSO (PU-PGSO) and Alcupol R4520 (PU-R4520). The internal structure of PU-PGSO and PU-R4520 was observed using a SEM (Fig. 5). The average cell size of PU-R4520 and PU-PGSO was found to be 0.511 and 50.805 μm, respectively, making the differences between both micrographs noticeable. Extra PU foams were synthesized using exclusively PGSO as biopolyol, but modifying up to ±10 wt.% the MDI, silicone, and water content. Nevertheless, the average cell size did not vary significantly from the previous value. This big difference in the internal structure might be justified by understanding the foaming
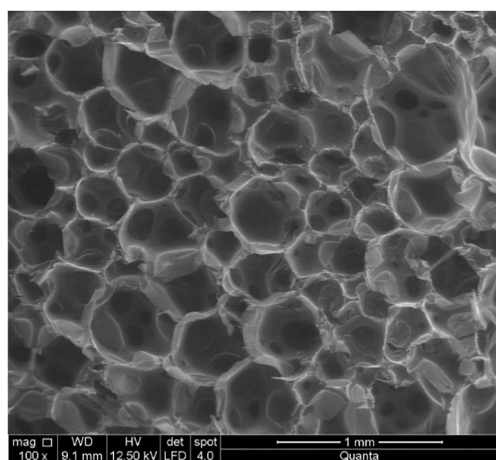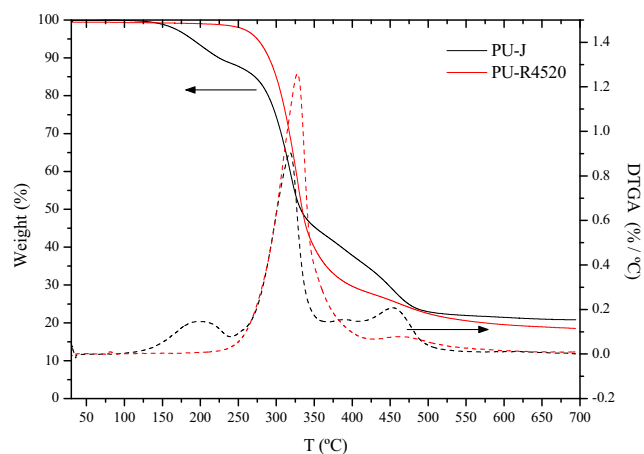
process, which is carried out because of two parallel processes: the formation of the polymeric structure and the gas production. If one of these processes is accelerated in comparison to the other, the morphology of the cell structure will be affected. Since the MW distribution and structure of both polyols are not similar, differences on the internal structure of PU foams might occur (Velencoso et al. 2015). However, the high influence of geometric shape and internal structure on the mechanical properties of PU foams has been demonstrated in literature (Goto et al. 2004; Hou et al. 2014). Therefore, PGSO cannot substitute totally Alcupol R4520 as polyol on the synthesis of rigid PU foams.

As neither of the phosphorylated biopolyols are suitable to fully replace Alcupol R4520, 13 different mixtures of the polyols (A to M) were used to synthesize rigid PU foams (PU-A to PU-M). These polyol mixtures are illustrated at Fig. 6 and the composition of each foam is shown in Table 2. A boundary condition of a hydroxyl value of 100 mg KOH/g, represented by the red line, was established to ensure the formation of a rigid PU foam in all cases.

Figure 6 shows the physical aspect of the rigid PU foams synthesized. As expected, differences among the foams were observed depending on the polyol mixture composition used on its synthesis. For example, when Alcupol R4520 was not used (PU-A and PU-D), an irregular foaming process was observed. However, a higher content on PGSO leaded to better-looking foam due to its higher hydroxyl value. The same trend was observed on the binary mixtures PGSO-Alcupol R4520 (PU-B and PU-H) and PMO-Alcupol R4520

Fig. 7 SEM image of foam PU-J

Table 3 Significant values of thermogravimetric analyses of PU-R4520 and PU-J

Sample	T_{on} (°C)	T_{max} (wt.%/°C)	Y_c (wt.%)
PU-R4520	274.8	318.5	18.2
PU-J	188.2	327.7	21.3

Fig. 9 SEM images of the chars at 700 °C of the foams **a** PU-R4520 and **b** PU-PGSO
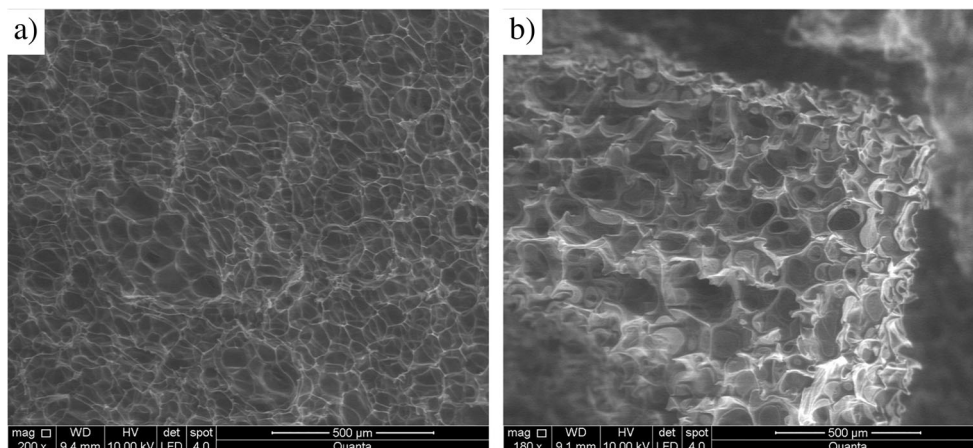
(PU-K, PU-L, and PU-M). It is also remarkable that the incorporation of small amounts of Alcupol R4520 to the polyol mixture improved notably the foaming process, as can be observed on PU-D, PU-E, and PU-K. Therefore, only the foams included on the highlighted region were considered for the subsequent analyses.

PU-J, synthesized from a polyol mixture of 43% Alcupol R4520, 17% PGSO, and 40% PMO, presented the most regular and similar to PU-R4520 internal structure. Figure 7 shows the SEM image of foam PU-J. As can be observed, it exhibited a polyhedral cell structure with faces formed by the junction of three struts. The average cell size was found to be 0.641 μm. Therefore, a rigid PU foam with a similar internal structure to a commercial one was synthesized substituting a 57% of the petroleum-based polyol by renewable phosphorylated biopolyols polyols.

Thermal degradation behavior of PU foams

It has been well recognized that phosphorus compounds can be used as flame retardants in polymers. The mechanism of flame retardancy of phosphoric groups, independently if they are covalently joined to the polymer chain or not, is based on the promotion of char formation and the inhibiting of glowing (Maiti et al. 1993).

TGA was used to investigate the effect of phosphate ester groups on the thermal stability of the rigid PU foams. Figure 8 shows the TGA and DTGA curves of PU-R4520 and PU-J. The significant values of the thermogravimetric analyses are resumed in Table 3, showing the onset degradation temperature (T_{on}), which is defined as the temperature at which a 5%

mass loss had occurred: the maximum rate degradation temperature (T_{max}) and the char yield at 700 °C (Y_c).

As can be observed, the foam PU-J showed a degradation trend at a lower temperature than PU-R4520, implying a lower onset degradation temperature. This behavior has been studied and attributed by some authors to the degradation of phosphorus groups, due to the fact that P–O–C bonds are less thermally stable than the predominant C–O–C bonds of petroleum-based polyether polyols (Mequanint et al. 2002; Troev et al. 1996). It is also remarkable that the weight loss of the phosphorylated PU foam (PU-J) in the temperature range of 360–410 °C is around 60% whereas for PU-R4520, an increase of about 70% was registered. This is caused by the degradation of the phosphate groups, which leads to the formation of an organophosphorus char that prevents degradation of the remaining PU foam (Liu et al. 2012a; Price et al. 2007). However, when the temperature raised to 430–490 °C, the foam PU-J undergoes another weight loss step, indicating the decomposition of organophosphorus char layer. Finally, the residue (Y_c) was observed to be higher in the foam PU-J than in the foam PU-R4520, indicating a protective effect of the char, even at 700 °C.

To confirm that the phosphorous compounds were retained in the char and thus acted as a flame retardant barrier, the morphological structure of the char was studied by SEM. EDAX associated with SEM was used to obtain the elemental composition of the chars of foams PU-R4520 and PU-J. Figure 9 shows the SEM images of both chars generated after thermogravimetric analysis at 700 °C. As can be observed, a great average cell size diminution was produced due to the thermal degradation process. Nevertheless, there is a more compact and denser structure on the surface of the burned PU-J, which indicates the presence of a protective char. Table 4 shows the surface composition of the chars obtained by EDAX. As can be observed, C, N, and O were the main remaining elements. Besides, PU-J showed a phosphorous content of 15.31 wt.%, confirming the formation of a protective phosphorylated layer, as also was corroborated by the TGA results.

Table 4 EDAX data of the chars of PU-R4520 and PU-J

Sample	C (wt.%)	N (wt.%)	O (wt.%)	P (wt.%)	Others (wt.%)
PU-R4520	51.93	22.82	24.04	0	1.21
PU-J	45.66	16.54	22.05	15.31	0.44

Conclusions

Grape seed oil (GSO) and methyl oleate (MO) were successfully epoxidized, reaching an oxirane oxygen content of 5.02 and 3.60%, respectively. The acid-catalyzed ring-opening hydrolysis was performed by using H_3PO_4 for both epoxidized materials, reaching a 100% conversion in 6 h. The formation of phosphate polyester was confirmed by FT-IR and ^{31}P-NMR. Unfortunately, it was not possible to synthesize a high-quality rigid PU foam using exclusively the previously synthesized phosphorylated biopolyols. The incorporation of small amounts of Alcupol R4520 to the polyol mixture improved notably the quality of the rigid PU foam. PU-J, synthesized from a polyol mixture of Alcupol R4520, PGSO, and PMO, having a composition of 43, 40, and 17 wt.%, respectively, presented the most regular and similar internal structure to the PU-R4520 foam. In addition, thermogravimetric and EDAX analyses revealed a noticeable improvement in PU thermal stability by the formation of a protective phosphorylated char layer.

References

Avar G, Meier-Westhues U, Casselmann H, Achten D (2012) Polyurethanes. Polymer science: a comprehensive reference, 10 volume set 10:411–441 doi:10.1016/B978-0-444-53349-4.00275-2

Bahattab MA, Donate-Robles J, García-Pacios V, Martín-Martínez JM (2011) Characterization of polyurethane adhesives containing nanosilicas of different particle size. Int J Adhes Adhes 31:97–103. doi:10.1016/j.ijadhadh.2010.11.001

Biswas A, Adhvaryu A, Gordon SH, Erhan SZ, Willett JL (2005) Synthesis of diethylamine-functionalized soybean oil. J Agric Food Chem 53:9485–9490. doi:10.1021/jf050731o

Chattopadhyay DK, Raju KVSN (2007) Structural engineering of polyurethane coatings for high performance applications. Prog Polym Sci 32:352–418. doi:10.1016/j.progpolymsci.2006.05.003

Chattopadhyay DK, Webster DC (2009) Thermal stability and flame retardancy of polyurethanes. Prog Polym Sci 34:1068–1133. doi:10.1016/j.progpolymsci.2009.06.002

Chokwe TB, Okonkwo JO, Sibali LL, Ncube EJ (2015) Alkylphenol ethoxylates and brominated flame retardants in water, fish (carp) and sediment samples from the Vaal River, South Africa. Environ Sci Pollut Res 22:11922–11929. doi:10.1007/s11356-015-4430-x

Da Porto C, Porretto E, Decorti D (2013) Comparison of ultrasound-assisted extraction with conventional extraction methods of oil and polyphenols from grape (Vitis Vinifera L.) seeds. Ultrason Sonochem 20:1076–1080. doi:10.1016/j.ultsonch.2012.12.002

de Haro JC, Izarra I, Rodríguez JF, Pérez Á, Carmona M (2016a) Modelling the epoxidation reaction of grape seed oil by peracetic acid. J Clean Prod 138:70–76. doi:10.1016/j.jclepro.2016.05.015

de Haro JC, Rodríguez JF, Pérez Á, Carmona M (2016b) Incorporation of azide groups into bio-polyols. J Clean Prod 138:77–82. doi:10.1016/j.jclepro.2016.05.012

Dinda S, Patwardhan AV, Goud VV, Pradhan NC (2008) Epoxidation of cottonseed oil by aqueous hydrogen peroxide catalysed by liquid inorganic acids. Bioresour Technol 99:3737–3744. doi:10.1016/j.biortech.2007.07.015

Findley TW, Swern D, Scanlan JT (1945) Epoxidation of unsaturated fatty materials with peracetic acid in glacial acetic acid solution. J Am Chem Soc 67:412–414. doi:10.1021/ja01219a018

Fiori L, Valbusa M, Lorenzi D, Fambri L (2012) Modeling of the devolatilization kinetics during pyrolysis of grape residues. Bioresour Technol 103:389–397. doi:10.1016/j.biortech.2011.09.113

Fridrihsone A, Stirna U, Lazdiņa B, Misane M, Vilsone D (2013) Characterization of polyurethane networks structure and properties based on rapeseed oil derived polyol. Eur Polym J 49:1204–1214. doi:10.1016/j.eurpolymj.2013.03.012

Goto A, Yamashita K, Nonomura C, Yamaguchi K (2004) Modeling of cell structure in polyurethane foam. J Cell Plast 40:481–488. doi:10.1177/0021955X04048422

Goud VV, Patwardhan AV, Pradhan NC (2006) Studies on the epoxidation of mahua oil (Madhumica indica) by hydrogen peroxide. Bioresour Technol 97:1365–1371. doi:10.1016/j.biortech.2005.07.004

Grishchuk S, Karger-Kocsis J (2011) Hybrid thermosets from vinyl ester resin and acrylated epoxidized soybean oil (AESO). Express Polym Lett 5:2–11. doi:10.3144/expresspolymlett.2011.2

Guo A, Cho Y, Petrović ZS (2000) Structure and properties of halogenated and nonhalogenated soy-based polyols. J Polym Sci A Polym Chem 38:3900–3910. doi:10.1002/1099-0518(20001101)38:21<3900::AID-POLA70>3.0.CO;2-E

Guo Y, Hardesty JH, Mannari VM, Massingill JL Jr (2007) Hydrolysis of epoxidized soybean oil in the presence of phosphoric acid. J Am Oil Chem Soc 84:929–935. doi:10.1007/s11746-007-1126-5

Hou C et al (2014) Mechanical response of hard bio-based PU foams under cyclic quasi-static compressive loading conditions. Int J Fatigue 59:76–89. doi:10.1016/j.ijfatigue.2013.09.012

Islam MR, Beg MDH, Jamari SS (2014) Development of vegetable-oil-based polymers. J Appl Polym Sci 131:9016–9028. doi:10.1002/app.40787

Ji D, Fang Z, He W, Zhang K, Luo Z, Wang T, Guo K (2015) Synthesis of soy-polyols using a continuous microflow system and preparation of soy-based polyurethane rigid foams. ACS Sustain Chem Eng 3:1197–1204. doi:10.1021/acssuschemeng.5b00170

Kim JW et al (2013) Organophosphorus flame retardants in house dust from the Philippines: occurrence and assessment of human exposure. Environ Sci Pollut Res 20:812–822. doi:10.1007/s11356-012-1237-x

Levchik SV, Weil ED (2006) A review of recent progress in phosphorus-based flame retardants. J Fire Sci 24:345–364. doi:10.1177/0734904106068426

Liu H, Xu K, Cai H, Su J, Liu X, Fu Z, Chen M (2012a) Thermal properties and flame retardancy of novel epoxy based on phosphorus-modified Schiff-base. Polym Adv Technol 23:114–121. doi:10.1002/pat.1832

Liu XQ, Huang W, Jiang YH, Zhu J, Zhang CZ (2012b) Preparation of a bio-based epoxy with comparable properties to those of petroleum-based counterparts. Express Polym Lett 6:293–298. doi:10.3144/expresspolymlett.2012.32

Lu H, Sun S, Bi Y, Yang G, Ma R, Yang H (2010) Enzymatic epoxidation of soybean oil methyl esters in the presence of free fatty acids. Eur J Lipid Sci Technol 112:1101–1105. doi:10.1002/ejlt.201000041

Maiti S, Banerjee S, Palit SK (1993) Phosphorus-containing polymers. Prog Polym Sci 18:227–261. doi:10.1016/0079-6700(93)90026-9

Matthäus B (2008) Virgin grape seed oil: is it really a nutritional highlight? Eur J Lipid Sci Technol 110:645–650. doi:10.1002/ejlt.200700276

Mequanint K, Sanderson R, Pasch H (2002) Thermogravimetric study of phosphated polyurethane ionomers. Polym Degrad Stab 77:121–128. doi:10.1016/S0141-3910(02)00088-5

Miao S, Wang P, Su Z, Zhang S (2014) Vegetable-oil-based polymers as future polymeric biomaterials. Acta Biomater 10:1692–1704. doi:10.1016/j.actbio.2013.08.040

Narine SS, Kong X, Bouzidi L, Sporns P (2007) Physical properties of polyurethanes produced from polyols from seed oils: II. Foams J Am Oil Chem Soc 84:65–72. doi:10.1007/s11746-006-1008-2

Ng TB, Bekhit AEDA, Fang EF, Wong JH (2015) Grape seed (Vitis vinifera) oils. In: Essential Oils in Food Preservation, Flavor and Safety. pp 455–462. doi:10.1016/B978-0-12-416641-7.00051-1

Pereira LC, de Souza AO, Bernardes MFF, Pazin M, Tasso MJ, Pereira PH, Dorta DJ (2015) A perspective on the potential risks of emerging contaminants to human and environmental health. Environ Sci Pollut Res 22:13800–13823. doi:10.1007/s11356-015-4896-6

Petrovic ZS (2008) Polyurethanes from vegetable oils. Polym Rev 48:109–155. doi:10.1080/15583720701834224

Petrović ZS, Ferguson J (1991) Polyurethane elastomers. Prog Polym Sci 16:695–836. doi:10.1016/0079-6700(91)90011-9

Petrović ZS, Guo A, Javni I, Cvetković I, Hong DP (2008) Polyurethane networks from polyols obtained by hydroformylation of soybean oil. Polym Int 57:275–281. doi:10.1002/pi.2340

Petrović ZS, Zhang W, Javni I (2005) Structure and properties of polyurethanes prepared from triglyceride polyols by ozonolysis. Biomacromolecules 6:713–719. doi:10.1021/bm049451s

Pretsch E, Bühlmann P, Affolter C (2000) Structure determination of organic compounds. Tables of Spectral Data. Chemical Laboratory Practice. Springer, Berlin. doi:10.1007/978-3-662-04201-4

Price D et al (2007) Thermal behaviour of covalently bonded phosphate and phosphonate flame retardant polystyrene systems. Polym Degrad Stab 92:1101–1114. doi:10.1016/j.polymdegradstab.2007.02.003

Samuelsson J, Jonsson M, Brinck T, Johtansson M (2004) Thiol-ene coupling reaction of fatty acid monomers. J Polym Sci A Polym Chem 42:6346–6352. doi:10.1002/pola.20468

Sharma BK, Liu Z, Adhvaryu A, Erhan SZ (2008) One-pot synthesis of chemically modified vegetable oils. J Agric Food Chem 56:3049–3056. doi:10.1021/jf073070z

Shinagawa FB, de Santana FC, Torres LRO, Mancini-Filho J (2015) Grape seed oil: a potential functional food? Food Sci Technol 35:399–406. doi:10.1590/1678-457X.6826

Simón D, Borreguero AM, De Lucas A, Rodríguez JF (2015) Glycolysis of viscoelastic flexible polyurethane foam wastes. Polym Degrad Stab 116:23–35. doi:10.1016/j.polymdegradstab.2015.03.008

Sovová H, Kučera J, Ježek J (1994) Rate of the vegetable oil extraction with supercritical CO2-II. Ext Grape Oil Chem Eng Sci 49:415–420. doi:10.1016/0009-2509(94)87013-6

Tavares LB, Boas CV, Schleder GR, Nacas AM, Rosa DS, Santos DJ (2016) Bio-based polyurethane prepared from Kraft lignin and modified castor oil. Express Polym Lett 10:927–940. doi:10.3144/expresspolymlett.2016.86

Troev K, Tsevi R, Bourova T, Kobayashi S, Uayama H, Roundhill DM (1996) Synthesis of phosphorus-containing polyurethanes without use of isocyanates. J Polym Sci A Polym Chem 34:621–631. doi:10.1002/(SICI)1099-0518(199603)34:4<621::AID-POLA8>3.0.CO;2-T

van der Veen I, de Boer J (2012) Phosphorus flame retardants: properties, production, environmental occurrence, toxicity and analysis. Chemosphere 88:1119–1153. doi:10.1016/j.chemosphere.2012.03.067

Velencoso MM, Ramos MJ, Serrano A, de Lucas A, Rodríguez JF (2015) Fire retardant functionalized polyol by phosphonate monomer insertion. Polym Int 64:1706–1714. doi:10.1002/pi.4970

Venkitasamy C, Teh HE, Atungulu GG, McHugh TH, Pan Z (2014) Optimization of mechanical extraction conditions for producing grape seed oil. Trans ASABE 57:1699–1705. doi:10.13031/trans.57.10570

Vroman I, Tighzert L (2009) Biodegradable polymers. Materials 2:307–344. doi:10.3390/ma2020307

Wu S, Soucek MD (1998) Oligomerization mechanism of cyclohexene oxide. Polymer 39:3583–3586. doi:10.1016/S0032-3861(97)10158-6

Zia KM, Bhatti HN, Ahmad Bhatti I (2007) Methods for polyurethane and polyurethane composites, recycling and recovery: a review. React Funct Polym 67:675–692. doi:10.1016/j.reactfunctpolym.2007.05.004